Tissue-based metabolomics profiling reveals metabolic signatures and major metabolic pathways of gastric cancer

Yaqin Wang
Henan Provincial People's Hospital
Wenchao Chen
Henan Provincial People's Hospital
Kun Li
Henan Provincial People's Hospital
Gang Wu (mri_1976@163.com)
Henan Provincial People's Hospital https://orcid.org/0000-0002-7305-9252
Wei Zhang
Henan Provincial People's Hospital
Peizhi Ma
Henan Provincial People's Hospital

Research Article

Keywords: Gastric cancer, Metabolomics, LC-MS/MS, Diagnostic biomarkers

DOI: https://doi.org/10.21203/rs.3.rs-326163/v1

Abstract

Purpose

This study was aimed to screen differential metabolites between gastric cancer (GC) and paracancerous (PC) tissues and find new biomarkers of GC.

Methods

GC (n = 28) and matched PC (n = 28) tissues were collected and LC-MS/MS analyses were performed to detect metabolites of GC and PC tissues in positive and negative models. Principal component analysis (PCA) and orthogonal projections to latent structures-discriminate analysis (OPLS-DA) were conducted to describe distribution of origin data and general separation and estimate the robustness and the predictive ability of our mode. Differential metabolites were screened based on criterion of variables with p value < 0.05 and VIP (variable importance in the projection) > 1.0. Receiver operating characteristic (ROC) analysis was performed to evaluate the diagnostic power of differential metabolites. Kyoto Encyclopedia of Genes and Genomes (KEGG) was performed to search for metabolite pathways and MetaboAnalyst was used for pathway enrichment analysis.

Results

Several metabolites were significantly changed in GC group compared with PC group. Thirteen metabolites with high VIP were chose and among which 1-methylnicotinamide, dodecanoic acid and sphinganine possessed high AUC values (AUC > 0.8) indicating an excellent discriminatory ability on GC. Pathways such as pentose phosphate pathway and histidine metabolism were focused based on differential metabolites demonstrating their effects on progress of GC.

Conclusions

In conclusion, we investigated the tissue-based metabolomics profile of GC and several differential metabolites and signaling pathways were focused. Further study is needed to verify those results.

Background

Gastric cancer (GC) is one of the most common malignant tumors, and ranked fifth as the cause of death among 36 cancers in the world (Bray et al. 2018). About 50% of cancer patients in China are gastrointestinal tumors, mainly for GC, and five-year survival rate is not more than 35% (Feng et al. 2019). GC shows a multistep progression (Wang et al. 2016). The 5-year survival rate of patients with advanced GC is less than 20%, while it may reach more than 90% that just invades mucosal or submucosal layer (Jung et al. 2014). However, most patients have reached middle and advanced stage by the time GC is found, which leads to a poor prognosis since GC has no specific clinical symptoms in the early stage. Therefore, it's important significantly to explore mechanism of GC and identify biomarkers for early diagnosis.

Metabolomics is a novel technique that explores biological states of metabolites among tissue extracts and body fluids such as plasma, serum and urine (Holmes et al. 2008; Nicholson et al. 2008) and has been used to characterize the metabolic disorders and identify potential biomarkers of various cancers (Cala et al. 2018; Chen et al. 2019; Denkert et al. 2008b). Studies on GC metabolomics were originate from plasma (Choi et al. 2016; Kuligowski et al. 2016; Lario et

al. 2017), serum (Corona et al. 2018; Liu et al. 2018), urine (Chan et al. 2016) samples mostly, but there are fewer studies related to GC tissues. Metabolic profiling of GC patients based on tissue samples with and without lymph node metastasis (LNM) was performed and some differential metabolites were identified as potential factors of diagnose and prognosis of GC patients with or without LNM (Zhang et al. 2018). This study was aimed to screen differential metabolites between GC and paracancerous (PC) tissues and identify potential biomarkers of GC.

Materials And Methods

Patient selection

Patients recruited in the study were diagnosed as GC according to results of gastroscope and biopsied. The inclusion and exclusion criteria were made. Inclusion criteria included: (□) aged between 20 and 80 years, both male or female; (□) primary tumor; (□) no treatment about cancer such as radiation, operation and chemoradiotherapy. Exclusion criteria were: (□) with metabolic disease including hyperlipoidemia, diabetes mellitus and gout; (□) with congenital diseases; (□) severe gastric cancer (survival < 2 months); (□) with distant metastases.

The study was approved by Ethics Committee of Henan Provincial People's Hospital and the registration number was ChiCTR2100041912.

Sample collection

GC and PC tissues were obtained from dissected specimens of patients receiving radical gastrectomy. Samples were washed off immediately with phosphate buffered saline and frozen in liquid nitrogen and stored at -80 °C.

Preparation of tissue extraction

Prior to analysis, 50 mg of sample was weighted and 1000 μL extract solution (acetonitrile: methanol: water = 2: 2: 1, with isotopically-labelled internal standard mixture) was added. After 30 s vortex, samples were grind at 35 Hz for 4 min and homogenized by sonicating for 5 min in ice-water bath, and then those steps were repeated for 3 times. Samples were incubated for 1 h at -40 ℃ and centrifuged at 12000 rpm for 15 min at 4 ℃. The supernatant was transferred to a fresh glass vial for analysis.

LC-MS/MS analysis

LC-MS/MS analyses were performed by an UHPLC system (Vanquish, Thermo Fisher Scientific) with an UPLC BEH amide column (2.1 mm * 100 mm, 1.7 μm) coupled to Q Exactive HFX mass spectrometer (Orbitrap MS, Thermo). Mobile phase was composed by water phase [25 mmol/L ammonium acetate and 25 ammonia hydroxide in water (pH = 9.75)] and acetonitrile (Shi et al. 2020) . The injection volume was 3ml and the auto-sampler temperature was 4 ℃. The Q Exactive HFX mass spectrometer was used to acquire MS/MS spectra on information-dependent acquisition (IDA) mode in the control of the acquisition software (Xcalibur, Thermo). In this mode, the acquisition software continuously evaluates the full scan MS spectrum. The ESI source conditions were set as following: sheath gas flow rate as 25 Arb, Aux gas flow rate as 20 Arb, capillary temperature 350 ℃, full MS resolution as 60000, MS/MS resolution as 7500, collision energy as 10/30/60 in NCE mode, spray Voltage as 3.6 kV (positive) or -3.2 kV (negative), respectively.

Data preprocessing and annotation

The original data were converted to the mzXML format by ProteoWizard and R package XCMS (version 3.2) (Kuhl et al. 2012), an in-house program, was used for peak detection, extraction, alignment, and integration. Then an in-house MS2

database (BiotreeDB, V2.1) was applied in metabolite annotation (Chen et al. 2020). The cutoff for annotation was set at 0.3.

Statistical analysis

The data were processed by SIMCA 16.0.2 software package (Sartorius Stedim Data Analytics AB, Umea, Sweden) (Chen et al. 2020; Triba et al. 2015) for principal component analysis (PCA) and orthogonal projections to latent structures-discriminate analysis (OPLS-DA). As an unsupervised pattern recognition method, PCA shows distribution of origin data and general separation and OPLS-DA was used to obtain maximal covariance between variables and sample category in both positive and negative models. 7-Fold cross-validation and 200 permutation tests were used to estimate the robustness and the predictive ability of our mode (Deng et al. 2019).

Variables with p value < 0.05 and VIP (variable importance in the projection) > 1.0 were defined as differential metabolites between GC and PC groups and results were presented by volcano plots. Box plots were made by ggplot2 function of R package. To further evaluate the diagnostic power of the potential biomarkers, receiver operating characteristic (ROC) analysis was carried out by plotROC function of R package and 95% confidence interval (CI) was calculated by pROC function.

Kyoto Encyclopedia of Genes and Genomes (KEGG) was performed to search for metabolite pathways and MetaboAnalyst was used for pathway enrichment analysis based on differential metabolites.

Results

Baseline clinical characteristics of patients

A total of 28 GC tissues and 28 matched tissues from the same patient were collected. There were 19 males and 9 females and their average age and BMI were 60±11 years and 21.6±2.7 kg/m^2. The rates of patients with smoking or drinking hobbies respectively were 53.6% and 35.7%.

Metabolic profiles of gastric cancer

An overview of study profile is showed in Fig 1. A total of 4893 peaks (negative ion mode: 2163, positive ion mode: 2730) were obtained and 485 metabolites (negative ion mode: 145, positive ion mode: 340) were identified. The UHPLC-QE-MS spectra examples of the same person were shown in Fig 2. There were some different mass spectrum peaks between GC and PC groups.

Examination of the PCA and OPLS-DA score plots (Fig 3a-3d) showed that most of samples were within 95% CI, but was failed to provide satisfactory separation of data. Permutation test of OPLS-DA models for the two groups were carried out to prevent overfit of models (Fig 3e and f). The abscissa represents correlation between random group and original group, and ordinate represents scores of R2Y and Q2. When permutation retention is 1, the values of Q2 and R2Y are close to 0.5 and 1 respectively, and Q2 is with positive slope showing that models have good predictability and do not overfit.

Potential biomarker analysis for discrimination

According to the criteria that p-value < 0.05 and VIP > 1, significantly differential metabolites between two groups were screened from all identified metabolites (Fig 4). There are 35 significantly different peaks (27 up-regulated and 8 down-regulated) in negative ion model, and 76 significantly different peaks (29 up-regulated and 47 down-regulated) in positive ion model existing in GC group compared with PC group.

Thirteen interestingly differential metabolites with high VIP values were chose and the differences in relative expression between two groups were shown in Fig 5 and table 1. Compared with PC group, seven high-expressed metabolites, including 1-methylnicotinamide, sphinganine, N-acetylputrescine, m-coumaric acid, imidazoleacetic acid, formiminoglutamic acid and gluconolactone were found in GC group. Meanwhile, six metabolites of dodecanoic acid, myo-inositol, D-glutamine, palmitoleic acid, carnosine and prostaglandin D2 were significantly lower expressed.

ROC analysis was conducted to estimate the diagnostic value of differential metabolites. All of selective metabolites showed nice ROC curves with high area under the curve (AUC) values (showed in table 1), among which 1-methylnicotinamide, dodecanoic acid and sphinganine possessed high AUC values (AUC>0.8) indicating an excellent discriminatory ability (Fig 6).

Pathway analysis of differential metabolites

Metabolic pathways on differential metabolites were analyzed by KEGG and MetaboAnalyst. As shown in Fig 7 and table 2, mainly five significantly altered pathways, namely histidine metabolism, alanine, aspartate and glutamate metabolism, sphingolipid metabolism, pentose phosphate pathway and cysteine and methionine metabolism, were revealed.

Discussion

In this study, we analyzed metabolic profiling of GC based on GC and PC tissues and found that some metabolites were significantly changed in GC group compared with PC group. Further analysis demonstrated that 1-methylnicotinamide, dodecanoic acid and sphinganine represented excellent clinical diagnostic capability for GC patients and some pathways were focused based on differential metabolites.

1-Methylnicotinamide (1-MNA), a metabolite of nicotinamide metabolic pathway, is transformed from N-methylation of nicotinamide conducted by nicotinamide N-methyltransferase (NNMT) and plays a key role in intracellular concentration of nicotinamide. Some researches described its effects about anti-inflammatory (Bryniarski et al. 2008), anti-thrombotic (Chlopicki et al.2007) and fibrinolytic (Mogielnicki et al. 2007). Tumor microenvironment derived 1-MNA contributes to immune modulation of T cells and represents a potential immunotherapy target to treat human cancer (Kilgour et al. 2021). However expression change of 1-MNA in cancer is still unknown, but the relationship between NNMT and cancers has been reported. Expression of NNMT was increased in multiple cancers, such as gastric cancer (Lim et al. 2006), lung cancer (Tomida et al. 2009) and colorectal cancer (Roessler et al. 2005). But Negative correlation was found between NNMT expression and size and progression of tumor suggesting that NNMT may have potential effect in an initial step of malignant conversion (Lu et al. 2018). 1-MNA was deemed to play a key role in mediating cellular actions of NNMT. So 1-MNA was likely to participate in the process of cancer. Our study illustrated the expression level of 1-MNA was significantly higher in GC tissues compared with PC tissues and owned excellent diagnostic capability for GC patients though mechanism is unclear.

Carnosine possessed inhibitory effects on growth of tumor cells and tumor cell glycolysis (Horii et al. 2012) that was associated with cellular mitochondrial bioenergetics (Cheng et al. 2019; Shen et al. 2014). Our study found that the level of carnosine was decreased in GC tissues compared with PC tissues that was corresponded to studies mentioned above. Histidine metabolism was enriched due to metabolites including carnosine, formiminoglutamic acid and imidazoleacetic acid. Histidine was identified as a potentially discriminant metabolite (Jing et al. 2018), and histidine metabolism was found in enrichment of functions and signaling pathways in patients with GC (Lario et al. 2017) illustrating that histidine metabolism was involved in progression of GC.

Prostaglandin D2 (PGD2), as an important metabolite of arachidonic acid (AA) metabolism, was showed to have antitumor effects (Iwanaga et al. 2014; Kim et al. 2005; Murata et al. 2011). A signaling pathway involved in PGD2 and PTGDR2 (prostaglandin D2 receptor 2) restricted the self-renewal of GC cells and suppressed tumor growth and metastasis indicating their effects on GC (Zhang et al. 2018a). Our study showed that the level of PGD2 was decreased in GC tissues compared with PC tissues verifying its anticancer effect (Zhang et al. 2018a) in terms of clinical samples. AA metabolism was enriched in our study and reported to play a key role in inflammation and tumorigenesis (Cuendet et al. 2000; Wang et al. 2010; Yarla et al. 2016). It has been evaluated as chemopreventive agent for tumor treatment by some inhibitory synthetic molecules (Brandao et al. 2013; Smalley et al. 1997).

Fatty acid biosynthesis pathway was focused due to dodecanoic acid and palmitoleic acid. Both of two metabolites were at relatively low level in GC tissues and dodecanoic acid showed nice diagnostic function on GC. Polyunsaturated fatty acid biosynthesis pathway has an effect on GC by determining ferroptosis sensitivity (Lee et al. 2020) that is associated with several pathological conditions including cancer (Li et al. 2020). Signal transduction and transcriptional activator 5A (STAT5A) promotes tumorigenesis of GC cells though reprograming fatty acid metabolism stating indirectly the relationship between fatty acid metabolism and tumorigenesis of GC (Dong et al. 2019). Fatty acid metabolism was enriched in a study about urinary metabolic profiling of GC (Liang et al. 2015) that is consistent with our results.

Pentose phosphate pathway (PPP) was deemed to participate in the progression and/or poor prognosis of GC (Wang et al. 2018; Yin et al. 2013). Rev-erbα, a nuclear receptor, inhibited proliferation of human gastric cancer cells by reducing glycolytic flux and PPP (Tao et al. 2019). As a controller of PPP, silencing of transketolase-like protein1 (TKTL1) inhibited proliferation of human GC cells in vitro and in vivo (Yuan et al. 2010). In this study, PPP was enriched and one of its metabolite, gluconolactone, was increased significantly in GC.

There are some limitations in the study. Firstly, the sample size was relatively small, although the GC and PC tissues were matched. Secondly, all patients were recruited from single center that might limit their generalization. Our study may be regarded as a preliminary study to explore metabolic characteristic of GC and PC tissues and further research with large sample, multiple research centers and verification in other omics technology was expected to confirm our results.

In conclusion, we investigated the tissue-based metabolomics profile of GC and several differential metabolites and signaling pathways were focused. Further study is needed to verify those results.

Declarations

Acknowledgments: This work was supported by National Natural Science Foundation of China (81803357).

Funding: This work was supported by National Natural Science Foundation of China (81803357).

Conflicts of interest/Competing interests: The authors declares that there is no conflict of interest.

Availability of data and material: Not applicable.

Code availability: Not applicable.

Authors' contributions: Not applicable.

Ethics approval: The study was approved by Ethics Committee of Henan Provincial People's Hospital and the registration number was ChiCTR2100041912.

Consent to participate: This study was exemption of informed consent because samples involved in the study were the remaining samples of other trials.

Consent for publication: Not applicable.

References

Brandao RD, Veeck J, Van de Vijver KK, Lindsey P, de Vries B, van Elssen CH, Blok MJ, Keymeulen K, Ayoubi T, Smeets HJ, Tjan-Heijnen VC, Hupperets PS (2013) A randomised controlled phase II trial of pre-operative celecoxib treatment reveals anti-tumour transcriptional response in primary breast cancer. Breast cancer research 15(2):R29. https://doi.org/10.1186/bcr3409

Bray F, Ferlay J, Soerjomataram I, Siegel RL, Torre LA, Jemal A (2018) Global cancer statistics 2018: GLOBOCAN estimates of incidence and mortality worldwide for 36 cancers in 185 countries. CA Cancer J Clin 68(6):394-424. https://doi.org/10.3322/caac.21492

Bryniarski K, Biedron R, Jakubowski A, Chlopicki S, Marcinkiewicz J (2008) Anti-inflammatory effect of 1-methylnicotinamide in contact hypersensitivity to oxazolone in mice; involvement of prostacyclin. Eur J Pharmacol 578(2-3):332-338. https://doi.org/10.1016/j.ejphar.2007.09.011

Cala MP, Aldana J, Medina J, Sanchez J, Guio J, Wist J, Meesters RJW (2018) Multiplatform plasma metabolic and lipid fingerprinting of breast cancer: A pilot control-case study in Colombian Hispanic women. PLoS One 13(2), e0190958. https://doi.org/10.1371/journal.pone.0190958

Chan AW, Mercier P, Schiller D, Bailey R, Robbins S, Eurich DT, Sawyer MB, Broadhurst D (2016) (1)H-NMR urinary metabolomic profiling for diagnosis of gastric cancer. Br J Cancer, 114(1), 59-62. https://doi.org/10.1038/bjc.2015.414

Chen L, Chang R, Pan S, Xu J, Cao Q, Su G, Zhou C, Kijlstra A, Yang P (2020) Plasma metabolomics study of Vogt-Koyanagi-Harada disease identifies potential diagnostic biomarkers. Exp Eye Res 196, 108070. https://doi.org/10.1016/j.exer.2020.108070

Chen PH, Cai L, Huffman K, Yang C, Kim J, Faubert B, Boroughs L, Ko B, Sudderth J, McMillan EA, et al (2019) Metabolic Diversity in Human Non-Small Cell Lung Cancer Cells. Mol Cell 76(5):838-851 e835. https://doi.org/10.1016/j.molcel.2019.08.028

Cheng JY, Yang JB, Liu Y, Xu M, Huang YY, Zhang JJ, Cao P, Lyu JX, Shen Y (2019) Profiling and targeting of cellular mitochondrial bioenergetics: inhibition of human gastric cancer cell growth by carnosine. Acta Pharmacol Sin 40(7):938-948. https://doi.org/10.1038/s41401-018-0182-8

Chlopicki S, Swies J, Mogielnicki A, Buczko W, Bartus M, Lomnicka M, Adamus J, Gebicki J (2007) 1-Methylnicotinamide (MNA), a primary metabolite of nicotinamide, exerts anti-thrombotic activity mediated by a cyclooxygenase-2/prostacyclin pathway. Br J Pharmacol 152(2):230-239. https://doi.org/10.1038/sj.bjp.0707383

Choi JM, Park WS, Song KY, Lee HJ, Jung BH (2016) Development of simultaneous analysis of tryptophan metabolites in serum and gastric juice - an investigation towards establishing a biomarker test for gastric cancer diagnosis. Biomed Chromatogr 30(12):1963-1974. https://doi.org/10.1002/bmc.3773

Corona G, Cannizzaro R, Miolo G, Caggiari L, De Zorzi M, Repetto O, Steffan A, De Re V (2018) Use of Metabolomics as a Complementary Omic Approach to Implement Risk Criteria for First-Degree Relatives of Gastric Cancer Patients. Int J

Mol Sci 19(3). https://doi.org/10.3390/ijms19030750

Cuendet M, Pezzuto JM (2000) The role of cyclooxygenase and lipoxygenase in cancer chemoprevention. Drug Metabol Drug Interact 17(1-4):109-157. https://doi.org/10.1515/DMDI.2000.17.1-4.109

Deng J, Xia Z, Qiu D, Jiao X, Xiao B, Zhou W, Yang H, Li J (2019) Nontarget metabolomics profiling of neuromyelitis optica spectrum disorder. Biomed Chromatogr 33(7), e4533. https://doi.org/10.1002/bmc.4533

Denkert C, Budczies J, Weichert W, Wohlgemuth G, Scholz M, Kind T, Niesporek S, Noske A, Buckendahl A, Dietel M et al (2008) Metabolite profiling of human colon carcinoma--deregulation of TCA cycle and amino acid turnover. Mol Cancer 7, 72. https://doi.org/10.1186/1476-4598-7-72

Dong SR, Ju XL, Yang WZ (2019) STAT5A reprograms fatty acid metabolism and promotes tumorigenesis of gastric cancer cells. Eur Rev Med Pharmacol Sci 23(19):8360-8370.

Feng RM, Zong YN, Cao SM, Xu RH (2019) Current cancer situation in China: good or bad news from the 2018 Global Cancer Statistics? Cancer Commun (Lond) 39(1), 22. https://doi.org/10.1186/s40880-019-0368-6

Holmes E, Wilson ID, Nicholson JK (2008) Metabolic phenotyping in health and disease. Cell 134(5):714-717. https://doi.org/10.1016/j.cell.2008.08.026

Horii Y, Shen J, Fujisaki Y, Yoshida K, Nagai K (2012) Effects of L-carnosine on splenic sympathetic nerve activity and tumor proliferation. Neurosci Lett 510(1):1-5. https://doi.org/10.1016/j.neulet.2011.12.058

Iwanaga K, Nakamura T, Maeda S, Aritake K, Hori M, Urade Y, Ozaki H, Murata T (2014) Mast cell-derived prostaglandin D2 inhibits colitis and colitis-associated colon cancer in mice. Cancer Res 74(11):3011-3019. https://doi.org/10.1158/0008-5472.CAN-13-2792

Jing F, Hu X, Cao Y, Xu M, Wang Y, Jing Y, Hu X, Gao Y, Zhu Z (2018). Discriminating gastric cancer and gastric ulcer using human plasma amino acid metabolic profile. IUBMB Life 70(6):553-562. https://doi.org/10.1002/iub.1748

Jung J, Jung Y, Bang EJ, Cho SI, Jang YJ, Kwak JM, Ryu DH, Park S, Hwang GS (2014) Noninvasive diagnosis and evaluation of curative surgery for gastric cancer by using NMR-based metabolomic profiling. Ann Surg Oncol 21 Suppl 4:S736-742. https://doi.org/10.1245/s10434-014-3886-0

Kilgour MK, MacPherson S, Zacharias LG, Ellis AE, Sheldon RD, Liu EY, Keyes S, Pauly B, Carleton G, Allard B et al (2021) 1-Methylnicotinamide is an immune regulatory metabolite in human ovarian cancer. Sci Adv 7(4). https://doi.org/10.1126/sciadv.abe1174

Kim J, Yang P, Suraokar M, Sabichi AL, Llansa ND, Mendoza G, Subbarayan V, Logothetis CJ, Newman RA, Lippman SM et al (2005) Suppression of prostate tumor cell growth by stromal cell prostaglandin D synthase-derived products. Cancer Res 65(14):6189-6198. https://doi.org/10.1158/0008-5472.CAN-04-4439

Kuhl C, Tautenhahn R, Bottcher C, Larson TR, Neumann S (2012) CAMERA: an integrated strategy for compound spectra extraction and annotation of liquid chromatography/mass spectrometry data sets. Anal Chem 84(1):283-289. https://doi.org/10.1021/ac202450g

Kuligowski J, Sanjuan-Herraez D, Vazquez-Sanchez MA, Brunet-Vega A, Pericay C, Ramirez-Lazaro MJ, Lario S, Gombau L, Junquera F, Calvet X et al (2016) Metabolomic Analysis of Gastric Cancer Progression within the Correa's Cascade

Using Ultraperformance Liquid Chromatography-Mass Spectrometry. J Proteome Res 15(8):2729-2738. https://doi.org/10.1021/acs.jproteome.6b00281

Lario S, Ramirez-Lazaro MJ, Sanjuan-Herraez D, Brunet-Vega A, Pericay C, Gombau L, Junquera F, Quintas G, Calvet X (2017) Plasma sample based analysis of gastric cancer progression using targeted metabolomics. Sci Rep 7(1), 17774. https://doi.org/10.1038/s41598-017-17921-x

Lee JY, Nam M, Son HY, Hyun K, Jang SY, Kim JW, Kim MW, Jung Y, Jang E, Yoon SJ et al (2020) Polyunsaturated fatty acid biosynthesis pathway determines ferroptosis sensitivity in gastric cancer. Proc Natl Acad Sci U S A 117(51):32433-32442. https://doi.org/10.1073/pnas.2006828117

Li J, Cao F, Yin HL, Huang ZJ, Lin ZT, Mao N, Sun B, Wang G (2020). Ferroptosis: past, present and future. Cell Death Dis, 11(2), 88. https://doi.org/10.1038/s41419-020-2298-2

Liang Q, Wang C, Li B (2015) Metabolomic Analysis Using Liquid Chromatography/Mass Spectrometry for Gastric Cancer. Appl Biochem Biotechnol 176(8):2170-2184. https://doi.org/10.1007/s12010-015-1706-z

Lim BH, Cho BI, Kim YN, Kim JW, Park ST, Lee CW (2006) Overexpression of nicotinamide N-methyltransferase in gastric cancer tissues and its potential post-translational modification. Exp Mol Med 38(5):455-465. https://doi.org/10.1038/emm.2006.54

Liu HN, Wu H, Tseng YJ, Chen YJ, Zhang DY, Zhu L, Dong L, Shen XZ, Liu TT (2018) Serum microRNA signatures and metabolomics have high diagnostic value in gastric cancer. BMC Cancer 18(1), 415. https://doi.org/10.1186/s12885-018-4343-4

Lu XM, Long H (2018) Nicotinamide N-methyltransferase as a potential marker for cancer. Neoplasma 65(5):656-663. https://doi.org/10.4149/neo_2018_171024N680

Mogielnicki A, Kramkowski K, Pietrzak L, Buczko W (2007) N-methylnicotinamide inhibits arterial thrombosis in hypertensive rats. J Physiol Pharmacol 58(3), 515-527.

Murata T, Aritake K, Matsumoto S, Kamauchi S, Nakagawa T, Hori M, Momotani E, Urade Y, Ozaki H (2011). Prostagladin D2 is a mast cell-derived antiangiogenic factor in lung carcinoma. Proc Natl Acad Sci U S A 108(49):19802-19807. https://doi.org/10.1073/pnas.1110011108

Nicholson JK, Lindon JC (2008) Systems biology: Metabonomics. Nature 455(7216):1054-1056. https://doi.org/10.1038/4551054a

Roessler M, Rollinger W, Palme S, Hagmann ML, Berndt P, Engel AM, Schneidinger B, Pfeffer M, Andres H, Karl J et al (2005) Identification of nicotinamide N-methyltransferase as a novel serum tumor marker for colorectal cancer. Clin Cancer Res, 11(18):6550-6557. https://doi.org/10.1158/1078-0432.CCR-05-0983

Shen Y, Yang J, Li J, Shi X, Ouyang L, Tian Y, Lu J (2014) Carnosine inhibits the proliferation of human gastric cancer SGC-7901 cells through both of the mitochondrial respiration and glycolysis pathways. PLoS One 9(8):e104632. https://doi.org/10.1371/journal.pone.0104632

Shi R, Zhang J, Fang B, Tian X, Feng Y, Cheng Z, Fu Z, Zhang J, Wu J (2020) Runners' metabolomic changes following marathon. Nutr Metab (Lond) 17, 19. https://doi.org/10.1186/s12986-020-00436-0

Smalley WE, DuBois RN (1997) Colorectal cancer and nonsteroidal anti-inflammatory drugs. Adv Pharmacol 39, 1-20. https://doi.org/10.1016/S1054-3589(08)60067-8

Tao L, Yu H, Liang R, Jia R, Wang J, Jiang K, Wang Z (2019) Rev-erbalpha inhibits proliferation by reducing glycolytic flux and pentose phosphate pathway in human gastric cancer cells. Oncogenesis 8(10), 57. https://doi.org/10.1038/s41389-019-0168-5

Tomida M, Mikami I, Takeuchi S, Nishimura H, Akiyama H (2009). Serum levels of nicotinamide N-methyltransferase in patients with lung cancer. J Cancer Res Clin Oncol 135(9):1223-1229. https://doi.org/10.1007/s00432-009-0563-y

Triba MN, Le Moyec L, Amathieu R, Goossens C, Bouchemal N, Nahon P, Rutledge DN, Savarin P (2015) PLS/OPLS models in metabolomics: the impact of permutation of dataset rows on the K-fold cross-validation quality parameters. Mol Biosyst 11(1) 13-19. https://doi.org/10.1039/C4MB00414K

Wang D, Dubois RN (2010). Eicosanoids and cancer. Nat Rev Cancer 10(3):181-193. https://doi.org/10.1038/nrc2809

Wang H, Zhang H, Deng P, Liu C, Li D, Jie H, Zhang H, Zhou Z, Zhao YL (2016) Tissue metabolic profiling of human gastric cancer assessed by (1)H NMR. BMC Cancer 16, 371. https://doi.org/10.1186/s12885-016-2356-4

Wang TA, Xian SL, Guo XY, Zhang XD, Lu YF (2018) Combined 18F-FDG PET/CT imaging and a gastric orthotopic xenograft model in nude mice are used to evaluate the efficacy of glycolysis-targeted therapy. Oncol Rep 39(1):271-279. https://doi.org/10.3892/or.2017.6060

Yarla NS, Bishayee A, Vadlakonda L, Chintala R, Duddukuri GR, Reddanna P, Dowluru KS (2016) Phospholipase A2 Isoforms as Novel Targets for Prevention and Treatment of Inflammatory and Oncologic Diseases. Curr Drug Targets 17(16):1940-1962. https://doi.org/10.2174/1389450116666150727122501

Yin L, Wang X, Luo C, Liu H, Zhang L, Zhang H, Zhang Y (2013). The value of expression of M2-PK and VEGF in patients with advanced gastric cancer. Cell Biochem Biophys, 67(3), 1033-1039. https://doi.org/10.1007/s12013-013-9601-0

Yuan W, Wu S, Guo J, Chen Z, Ge J, Yang P, Hu B, Chen Z (2010) Silencing of TKTL1 by siRNA inhibits proliferation of human gastric cancer cells in vitro and in vivo. Cancer Biol Ther 9(9):710-716. https://doi.org/10.4161/cbt.9.9.11431

Zhang B, Bie Q, Wu P, Zhang J, You B, Shi H, Qian H, Xu W (2018) PGD2/PTGDR2 Signaling Restricts the Self-Renewal and Tumorigenesis of Gastric Cancer. Stem Cells 36(7):990-1003. https://doi.org/10.1002/stem.2821

Zhang H, Cui L, Liu W, Wang Z, Ye Y, Li X, Wang H (2018) (1)H NMR metabolic profiling of gastric cancer patients with lymph node metastasis. Metabolomics 14(4), 47. https://doi.org/10.1007/s11306-017-1293-9

Tables

Table 1 Major differential metabolites between GC and PC groups

NO	Metabolites	Regulation	Polarity	VIP	P value	Fold chang	AUC	95% CI	Metabolism pathways
1	1-Methylnicotinamide	Up	POS	2.89	0.0000	0.30	0.904	0.823-0.986	Nicotinate and nicotinamide metabolism
2	Sphinganine	Up	POS	2.45	0.0042	0.22	0.847	0.748-0.946	Sphingolipid metabolism
3	N-Acetylputrescine	Up	POS	2.44	0.0125	0.34	0.760	0.630-0.890	Arginine and proline metabolism
4	Dodecanoic acid	Down	NEG	2.31	0.0000	2.07	0.856	0.749-0.963	Fatty acid biosynthesis
5	myo-Inositol	Down	NEG	2.29	0.0003	1.70	0.777	0.653-0.900	No
6	D-Glutamine	Down	NEG	2.06	0.0069	1.24	0.724	0.588-0.861	No
7	m-Coumaric acid	Up	NEG	2.04	0.0011	0.60	0.728	0.594-0.862	Phenylalanine metabolism
8	Imidazoleacetic acid	Up	NEG	2.01	0.0459	0.44	0.689	0.539-0.839	Histidine metabolism
9	Palmitoleic acid	Down	NEG	1.47	0.0019	2.01	0.767	0.638-0.895	Fatty acid biosynthesis
10	Formiminoglutamic acid	Up	POS	1.45	0.0435	0.57	0.649	0.501-0.797	Histidine metabolism
11	Carnosine	Down	POS	1.45	0.0131	2.08	0.716	0.578-0.853	Histidine metabolism
12	Gluconolactone	Up	NEG	1.36	0.0352	0.81	0.661	0.515-0.807	Pentose phosphate pathway
13	Prostaglandin D2	Down	NEG	1.15	0.0055	2.66	0.723	0.587-0.859	Arachidonic acid metabolism

AUC: area under the ROC curve; Fold change: PC group *vs* GC group.

Table 2 Detailed results of pathway analyses based on metabolomics data.

No.	Pathway	Total	Hits	Raw p	-ln(p)	Hits names	Impact
1	Sphingolipid metabolism	25	2	0.05	2.94	Sphinganine Sphingosine	0.23
2	Histidine metabolism	44	3	0.03	3.62	Formiminoglutamic acid Carnosine Imidazoleacetic acid	0.07
3	Alanine, aspartate and glutamate metabolism	24	2	0.05	3.02	N-Acetyl-L-aspartic acid; Succinic acid semialdehyde	0.06
4	Cysteine and methionine metabolism	56	1	0.57	0.55	5'-Methylthioadenosine	0.05
5	Pentose phosphate pathway	32	1	0.38	0.96	Gluconolactone	0.04
6	Arachidonic acid metabolism	62	2	0.24	1.44	Prostaglandin D2 Prostaglandin B2	0.03
7	Butanoate metabolism	40	1	0.46	0.79	Succinic acid semialdehyde	0.03
8	Pentose and glucuronate interconversions	53	1	0.55	0.59	D-Xylitol	0.03
9	Phenylalanine metabolism	45	1	0.50	0.70	m-Coumaric acid	0.03
10	Pyrimidine metabolism	60	1	0.60	0.51	Cytidine	0.03
11	beta-Alanine metabolism	28	1	0.35	1.06	Carnosine	0.02
12	Nicotinate and nicotinamide metabolism	44	2	0.14	1.97	NAD 1-Methylnicotinamide	0.02
13	Glycerophospholipid metabolism	39	2	0.11	2.17	Triethanolamine Glycerophosphocholine	0.01
14	Tyrosine metabolism	76	1	0.69	0.37	Succinic acid semialdehyde	0.00
15	Arginine and proline metabolism	77	1	0.69	0.37	N-Acetylputrescine	0.00
16	Purine metabolism	92	1	0.76	0.28	Deoxyinosine	0.00
17	Fatty acid biosynthesis	49	2	0.17	1.80	Dodecanoic acid Palmitoleic acid	0.00
18	Linoleic acid metabolism	15	1	0.20	1.60	Bovinic acid	0.00
19	Ether lipid metabolism	23	1	0.29	1.22	Glycerophosphocholine	0.00
20	Vitamin B6 metabolism	32	1	0.38	0.96	Succinic acid semialdehyde	0.00
21	Steroid hormone biosynthesis	99	1	0.78	0.25	Cholesterol sulfate	0.00

Hits: the matched number of metabolites in one pathway. Raw P: the original P value calculated from the enrichment analysis. Hits names: names about the matched differential metabolites in one pathway.

Figures

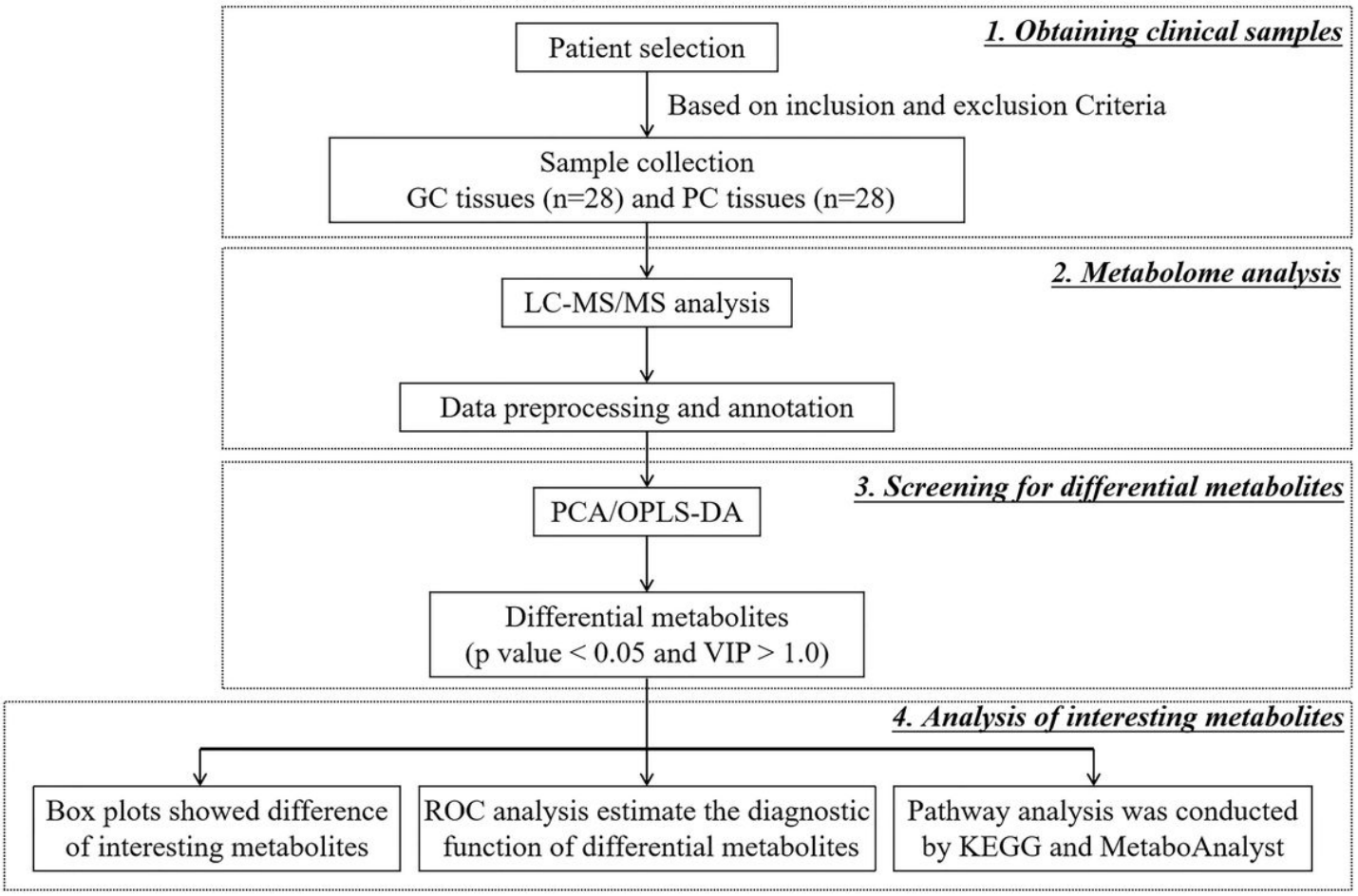

Figure 1

An overview of study profile for identifying metabolites of GC

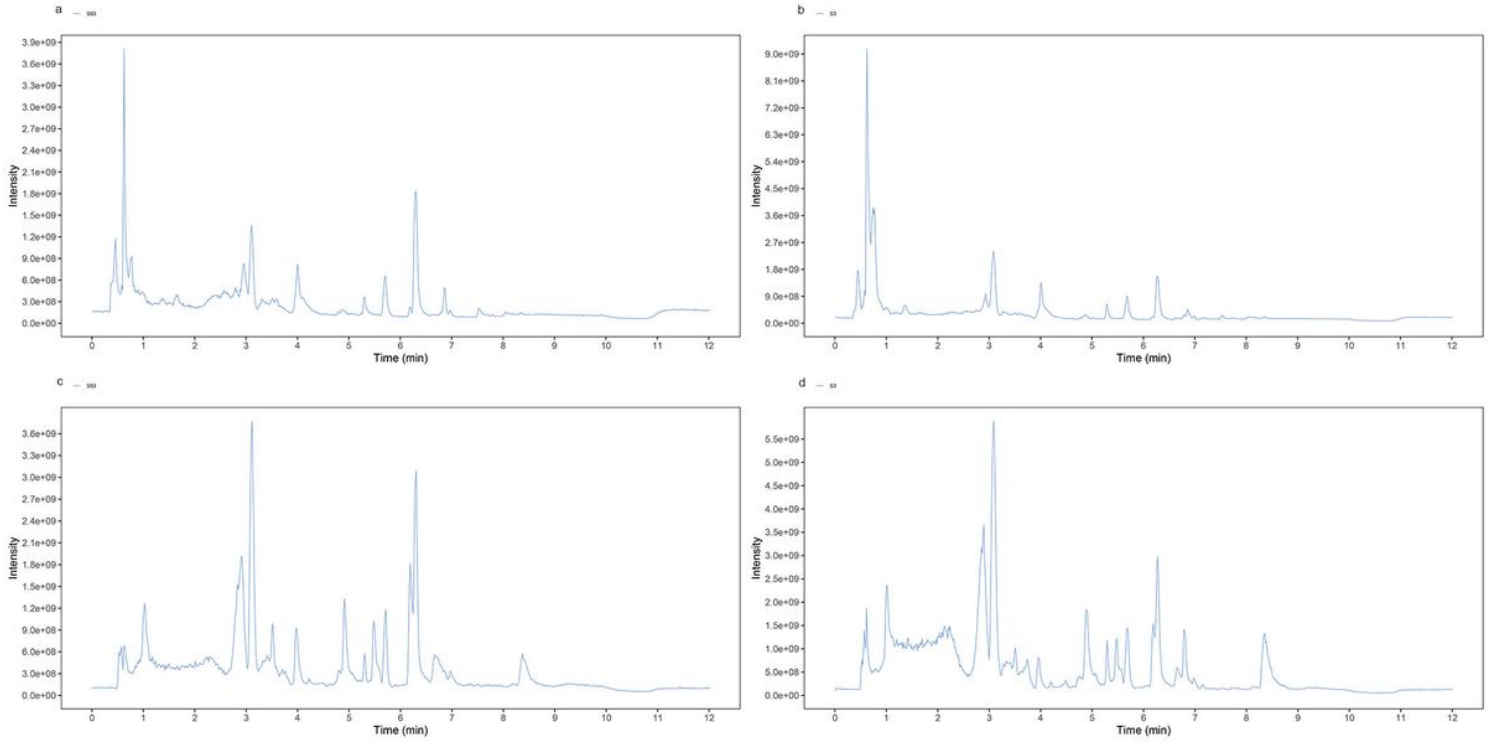

Figure 2

Representative UHPLC-QE-MS total ion chromatograms of GC and PC tissue. Negative ion mode of GC tissue (A) and PC tissue (B), and positive ion mode of GC tissue (C) and PC tissue (D) of the same patient

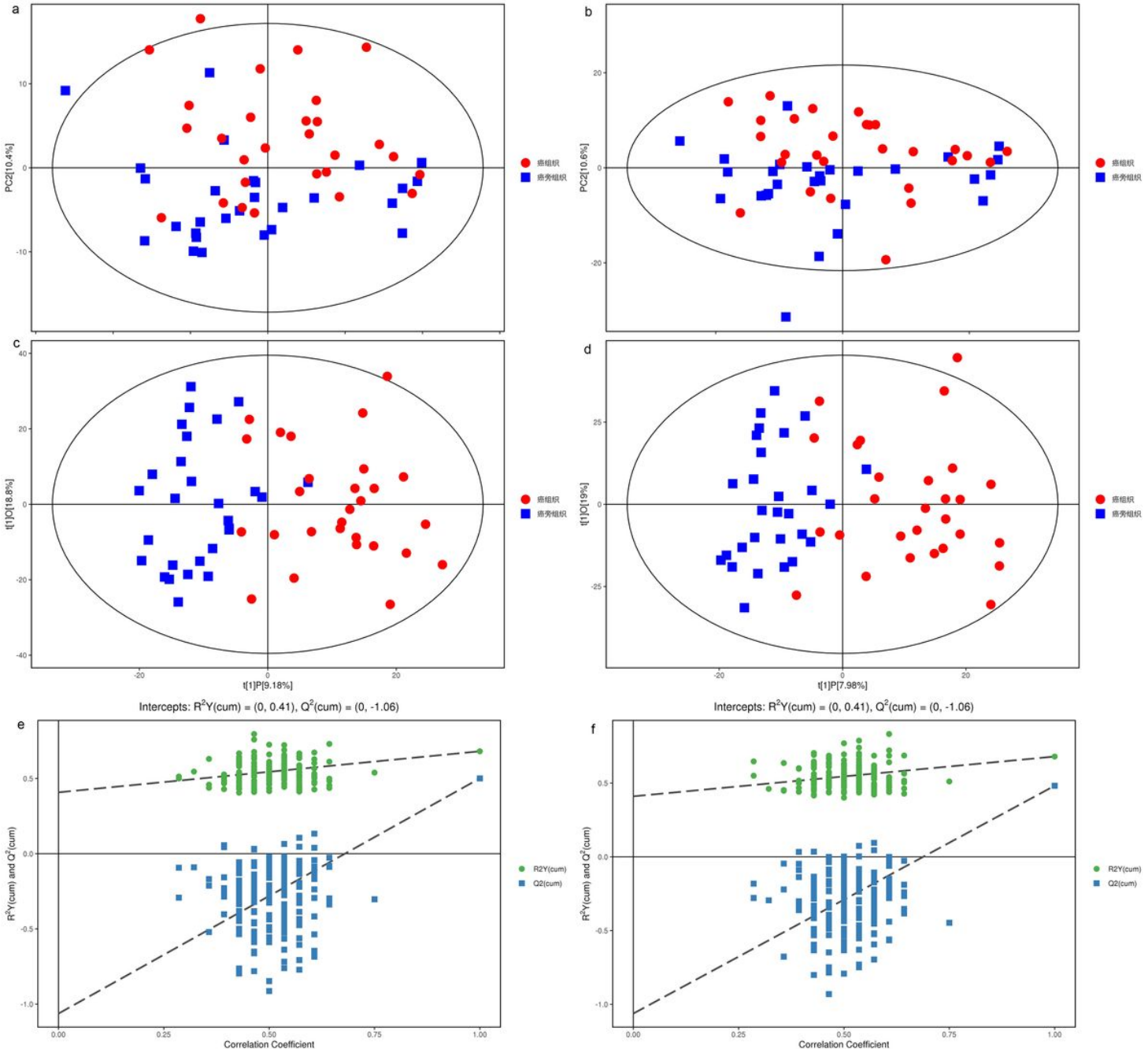

Figure 3

Identification of discriminating biomarkers by metabolome analysis. The PCA (A) and OPLS-DA (C) score plot and OPLS-DA (E) model are in negative ion mode. PCA (B) and OPLS-DA (D) score plot and OPLS-DA (F) model are in positive ion mode

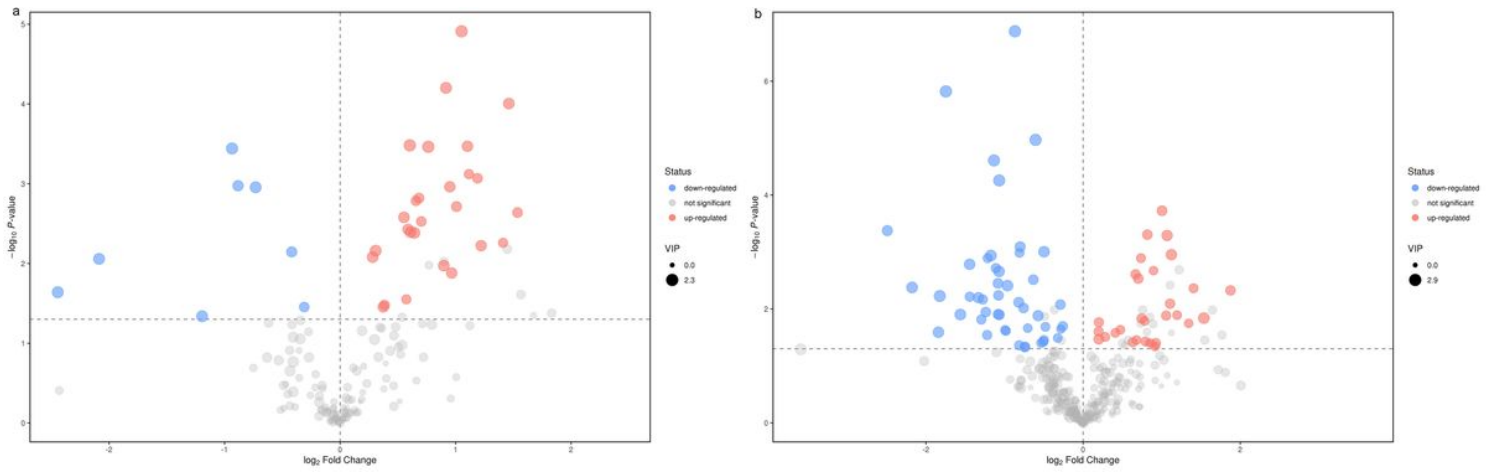

Figure 4

Volcano plots for the GC vs. PC groups. A was derived from negative ion mode of GC patients. B was derived from positive ion mode of GC patients

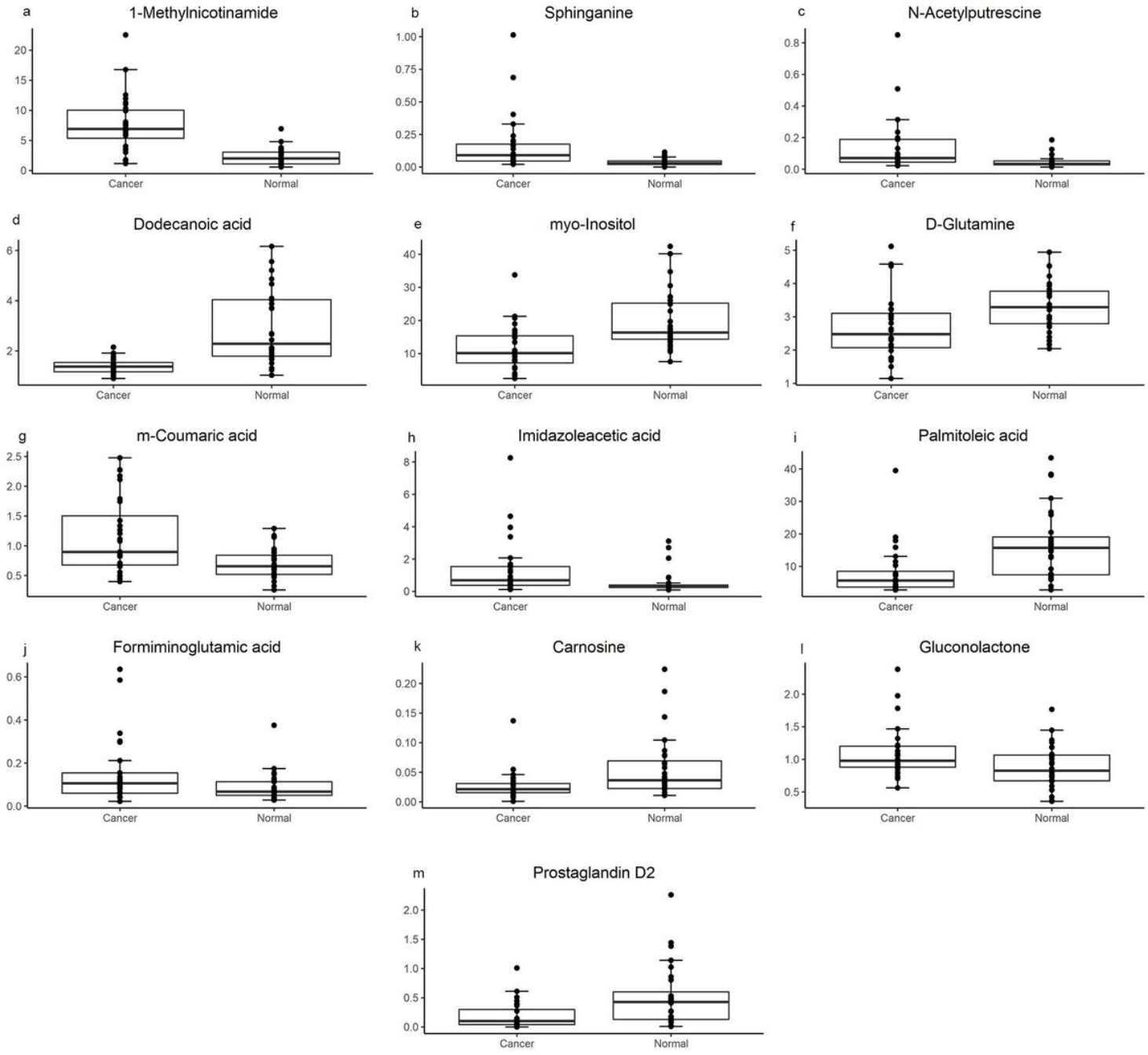

Figure 5

Relative intensity of the significantly altered metabolites

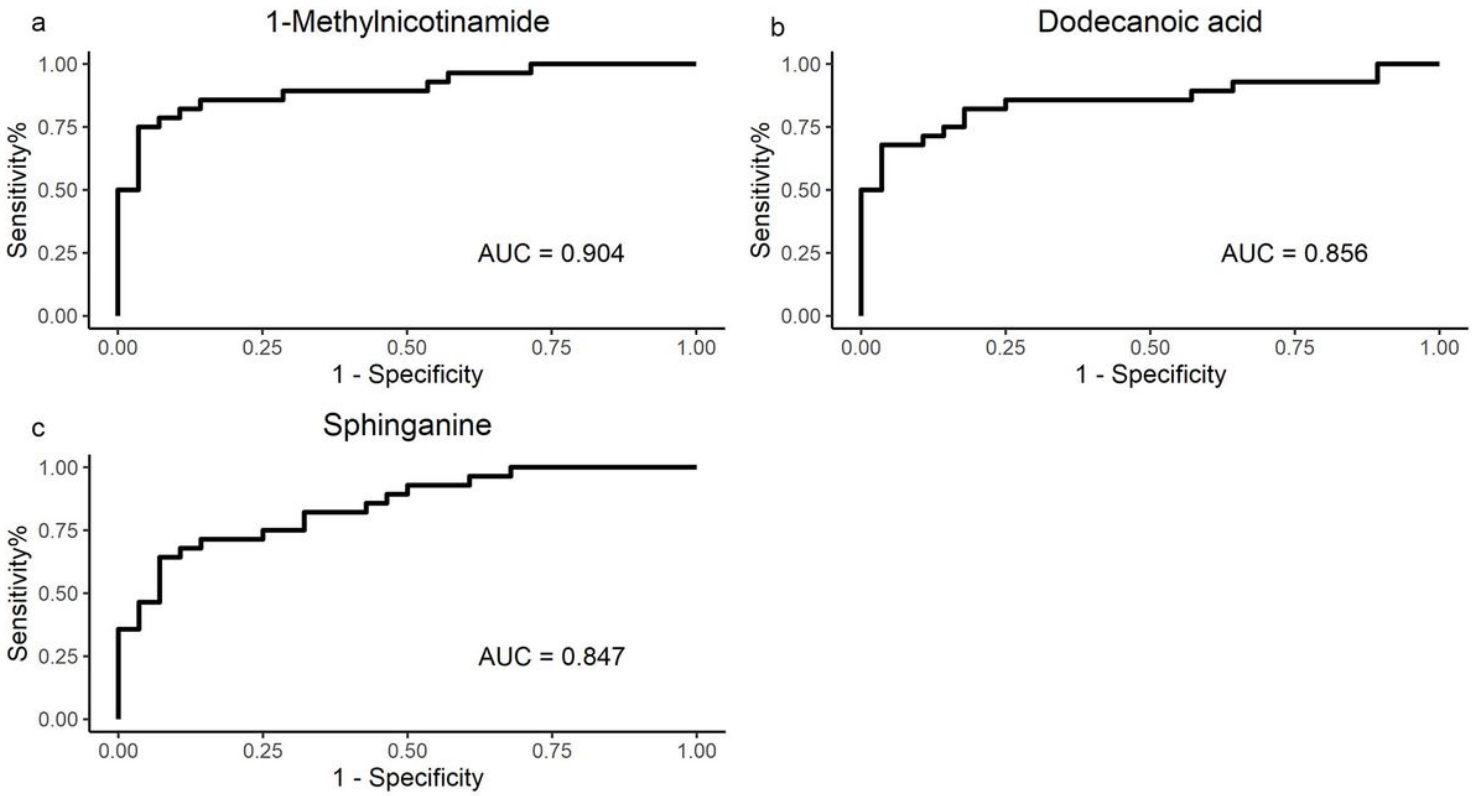

Figure 6

ROC graphs of metabolites with the high AUC values. A: 1-methylnicotinamide; B: dodecanoic acid; C: sphinganine

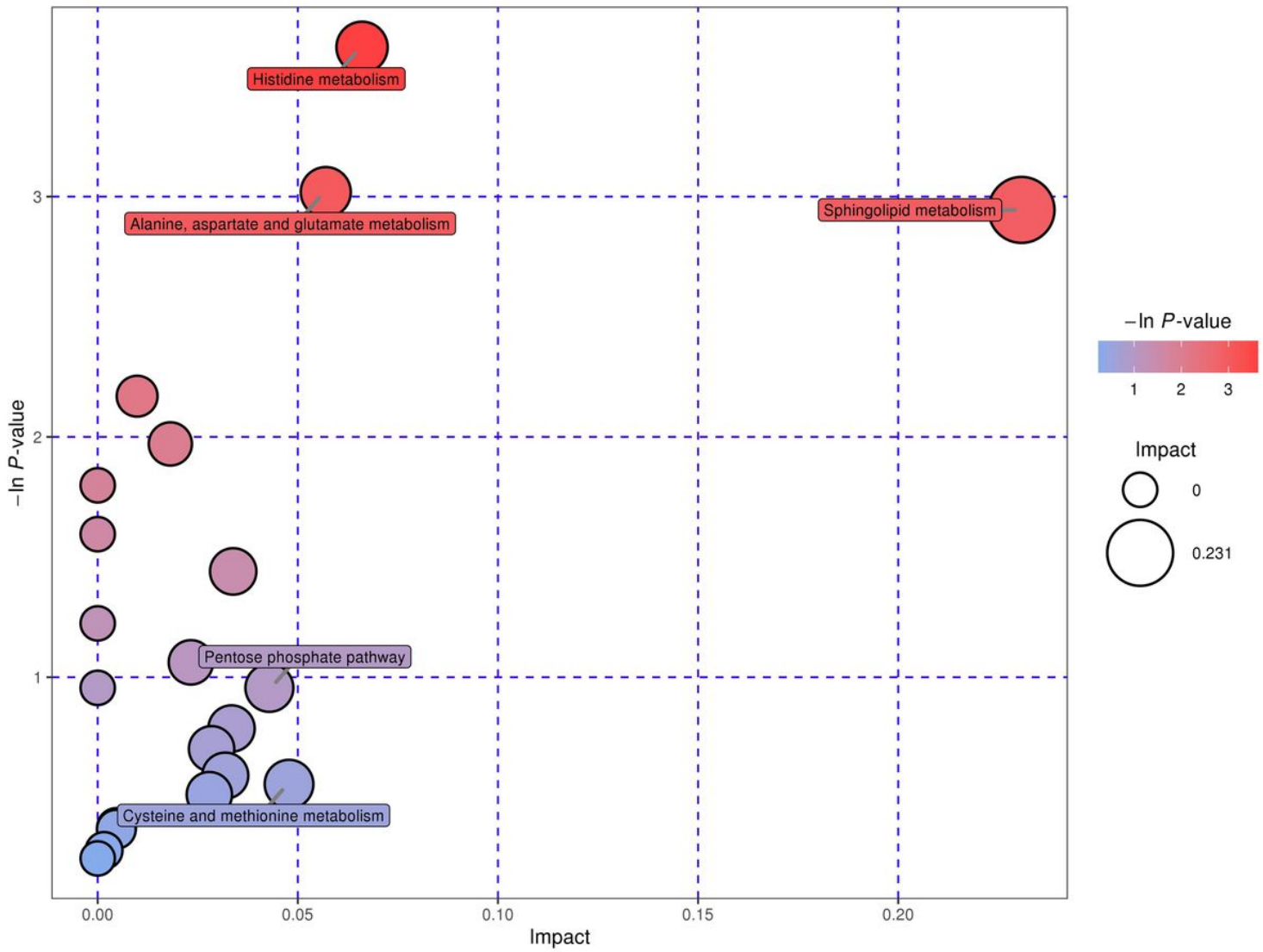

Figure 7

Bubble analysis of metabolic pathways between GC and PC groups